

## Chaos in Robert Hooke's inverted cone

BY MÉDÉRIC ARGENTINA<sup>1,2</sup>, PIERRE COULLET<sup>1,2</sup>, JEAN-MARC GILLI<sup>1,2</sup>,  
MARC MONTICELLI<sup>1,2</sup> AND GERMAIN ROUSSEAU<sup>1,2,\*</sup>

<sup>1</sup>*Université de Nice-Sophia Antipolis, Institut Non-Linéaire de Nice, UMR 6618  
CNRS-UNICE, 1361, route des Lucioles, 06560 Valbonne, France*

<sup>2</sup>*Université de Nice-Sophia Antipolis, Institut Robert Hooke, Parc Valrose,  
06108 Nice Cedex 2, France*

Robert Hooke is perhaps one of the first scientists to have met chaotic motions. Indeed, to invert a cone and let a ball move in it was a mechanical model used by him to mimic the motion of a planet around a centre of force like the Sun. However, as the cone is inclined with respect to the gravity field, the perfect rosace followed by the particle becomes chaotic meanderings. We revisit this classical experiment designed by Hooke with the modern tools of dynamical systems and chaos theory. By a combination of both numerical simulations and experiments, we prove that the scenario of transition to the chaotic behaviour is through a period-doubling instability.

**Keywords:** chaos; mechanics; Hooke; inverted cone; ball

### 1. Introduction

Since the time of Kepler, the laws describing the elliptic paths of the planets around the Sun were known. However, one must wait for the Principia of Newton in order to establish their universality. Indeed, the Englishman introduced the concept of central force in the resolution of the problem. However, Robert Hooke was the first to envisage the design of simple experiments with pendula, presented to the Royal Academy in order to understand the planetary orbits of the Solar System (Patterson 1952; Gal 1996; Nauenberg 2005*a, b*): ‘This inflection of a direct motion into a curve by a supervening attractive principle I endeavour to explicate from some experiments with a pendulous body... Circular motion [of the pendulum] is compounded of an endeavour by a direct motion by the tangent, and of another endeavour tending to the centre’. In addition, Hooke designed an inverted cone in which he launched a spherical ball assuming no friction. The mass is attracted by the centre, whereas the geometrical curvature tends to move away the ball from the rest position. Hooke noticed that the ‘planet’ represented by the mass was compelled to follow a rosace-like trajectory around the centre (the Sun). He mentioned his observation of regular motion in a letter to Isaac Newton in 1679 (Nauenberg 2005*a, b*), but there is no clear evidence that he presented this set-up to the Royal Society.

\* Author for correspondence (germain.rousseau@inln.cnrs.fr).

The motion inside the inverted cone is a particular case of the motion of a body on a given surface (Routh 1898). The inverted cone is an oscillator which is nonlinear due to its geometry. Lopez-Ruiz & Pacheco have given a very good account of the different types of trajectories inside the cone depending on the initial conditions (Lopez-Ruiz & Pacheco 2002a,b, 2005). Indeed, the system of equations describing the motion is completely integrable when the direction of gravity is along the vertical of the cone. As a matter of fact, this system has two degrees of freedom: four generalized coordinates in phase space  $s, \dot{s}, \phi, \dot{\phi}$  ( $s$  is the coordinate along a generatrix of the cone and the angle  $\phi$  indicates its azimuthal position) minus the conservation of energy and the conservation of angular momentum ( $4 - 1 - 1 = 2$ ). If one inclines the cone with respect to the direction of gravity, one loses the conservation of angular momentum and ends up with three degrees of freedom. As a consequence, chaos can appear as explained in the classic book by Bergé et al. (1984).

In this work, we revisit the classical work of Robert Hooke on the inverted cone with the modern viewpoint of chaotic dynamics. In particular, we show that the scenario of transition to chaos is through a period-doubling instability.

## 2. Euler–Lagrange equations

Let suppose that a rigid sphere (located at  $(x, y, z)$ ) is rolling on a surface that is defined by

$$z = f(x, y) = \tan \alpha \sqrt{\epsilon^2 + (x^2 + y^2)}, \quad (2.1)$$

where  $\epsilon$  has the dimension of a length (see below). We will treat the body as point-like mass and will not include its rotational kinetic energy. So, we will denote it as a sliding point particle. The equation of the surface has two asymptotic limits. Far away from the origin,

$$z \sim \tan \alpha \sqrt{x^2 + y^2},$$

the surface tends to be a cone with the revolution axis being  $z$  and the aperture angle  $\alpha$ . The other limit is reached when  $r \ll \epsilon$ ,

$$z \sim \tan \alpha \left( \epsilon + \frac{r^2}{2\epsilon} \right).$$

Thus,  $\epsilon$  measures the distance from the origin over which the surface is parabolic. When  $\epsilon$  is zero, the surface is exactly a cone. We chose to include a parabolic shape near the origin to remove any shock of the sphere with the surface: if the radius of the sphere is smaller than the radius of the parabola  $\epsilon$ , shocks will be avoided as shown in figure 1.

We now derive the equations that describe the dynamics of the particle. The ball has a mass  $m$  and is located with the coordinates  $(x, y, z)$ . We suppose that the gravity field is tilted with respect to the axis of symmetry of the cone, with an angle  $\theta$ . We use the Lagrangian approach to obtain the equations. The kinetic energy  $T$  is

$$T = \frac{1}{2} m (\dot{x}^2 + \dot{y}^2 + \dot{z}^2).$$

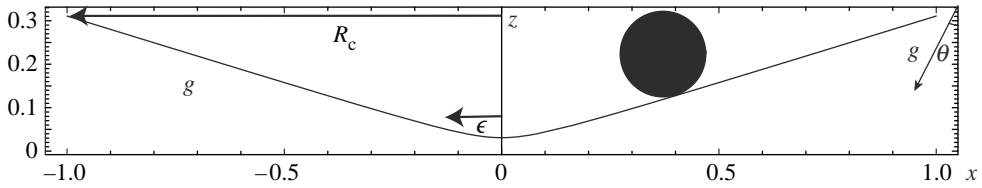


Figure 1. Shape of the cone obtained with  $\epsilon=0.1$  and  $\alpha=0.3$ . Here, the radius of the sphere is 0.05 and no shock is expected when its mass centre approaches the origin.

The potential energy  $U$  is purely gravitational and is written as

$$U = mg(\sin \theta x + \cos \theta z),$$

and it is then understood that the symmetry axis of the cone makes an angle  $\theta$  with the gravity. Finally, since the particle is constrained to move on the cone, we need to add a Lagrangian multiplier  $\lambda$  that represents the force exerted by the cone in order to maintain the particle on its boundary (José & Saletan 1998). We deduce the Lagrangian

$$L = T - U - \lambda(z - f(x, y)),$$

$$L = \frac{1}{2} m(\dot{x}^2 + \dot{y}^2 + \dot{z}^2) - mg(\sin \theta x + \cos \theta z) - \lambda \left( z - \tan \alpha \sqrt{\epsilon^2 + (x^2 + y^2)} \right).$$

By variations, we then get the Euler–Lagrange equations for  $x$ ,  $y$  and  $z$ ,

$$m\ddot{x} = \frac{\tan \alpha \lambda x}{\sqrt{\epsilon^2 + x^2 + y^2}} - mg \sin \theta, \tag{2.2}$$

$$m\ddot{y} = \frac{\tan \alpha \lambda y}{\sqrt{\epsilon^2 + x^2 + y^2}}, \tag{2.3}$$

$$m\ddot{z} = -\lambda - mg \cos \theta. \tag{2.4}$$

Then it becomes clear that the time-dependent Lagrange multiplier is the  $z$  component of the force which maintains the particle on the cone. Before going further, we set the system in a non-dimensional form,

$$\ddot{x} = \tan \alpha \frac{\lambda}{\sqrt{\rho^2 + x^2 + y^2}} x - \tan \theta, \tag{2.5}$$

$$\ddot{y} = \tan \alpha \frac{\lambda}{\sqrt{\rho^2 + x^2 + y^2}} y, \tag{2.6}$$

$$\ddot{z} = -\lambda - 1, \tag{2.7}$$

where  $\rho = (\epsilon/R_c)$  is the dimensionless radius of the parabolic regularization of the cone at the origin and  $R_c$  is the radius of the cone seen from above. In order to have compact equations, we use complex variables and by denoting  $A = x + iy$ , the complex amplitude of the oscillation in the  $(x, y)$  plane, we then deduce

$$\ddot{A} = \frac{\lambda \tan \alpha}{\sqrt{\rho^2 + |A|^2}} A - \tan \theta, \tag{2.8}$$

$$\ddot{z} = -\lambda - 1. \tag{2.9}$$

We need to compute  $\lambda$ . Taking the second derivative of the cone equation (2.1) with respect to time, we find the following relation:

$$\ddot{z} + \tan \alpha \frac{(x\dot{x} + y\dot{y})^2}{(\rho^2 + x^2 + y^2)^{3/2}} - \tan \alpha \frac{(x^2 + y^2 + x\ddot{x} + y\ddot{y})}{\sqrt{\rho^2 + x^2 + y^2}} = 0. \tag{2.10}$$

Then, by using equations (2.9) and (2.10), we compute  $\lambda$  as a function of  $x$  and  $y$ . We employ the definition of  $A$  and equation (2.8) to get

$$\lambda = \frac{1}{1 + \tan^2 \alpha \frac{|A|^2}{\rho^2 + |A|^2}} \left( -1 + \tan \alpha \tan \theta \frac{A + \bar{A}}{2\sqrt{\rho^2 + |A|^2}} + \tan \alpha \left( \frac{(\partial_t |A|^2)^2}{4(\rho^2 + |A|^2)^{3/2}} - \frac{|\partial_t A|^2}{\sqrt{\rho^2 + |A|^2}} \right) \right). \tag{2.11}$$

### 3. The limit of a flat cone

In the limit of a very flat cone,  $\tan \alpha \ll 1$ , the Lagrange multiplier is extremely simple and becomes  $\lambda = -1$  as seen from equation (2.11). The equation for the complex amplitude  $A$  is

$$\ddot{A} = - \frac{\tan \alpha}{\sqrt{\rho^2 + |A|^2}} A - \tan \theta.$$

By using a convenient time-scale, only two control parameters remain:  $\mu$  defined to be the ratio between the slope of the cone and the slope of the inclination  $\tan \theta / \tan \alpha$ , and  $\rho$  the dimensionless curvature radius of the cone near the origin.

$$\ddot{A} = - \frac{A}{\sqrt{\rho^2 + |A|^2}} - \mu, \tag{3.1}$$

is a fourth-order ordinary differential equation (since  $A$  is complex and derived twice) satisfying the conservation of the energy  $\kappa$ ,

$$\kappa = |\dot{A}|^2 - 2\sqrt{\rho^2 + |A|^2} + \mu(A + \bar{A}). \tag{3.2}$$

It is then an equivalent of a third-order ODE. When the cone is not tilted with respect to the gravity field  $\mu = 0$ , the typical solution is a rosace-like oscillation. By setting  $A = r e^{i\phi}$ , we obtain the following two equations:

$$\ddot{r} = - \frac{r}{\sqrt{\rho^2 + r^2}} + \frac{J^2}{r^3}, \tag{3.3}$$

$$J = r^2 \dot{\phi}, \tag{3.4}$$

where  $J$  is the initial angular momentum when the ball is released on the cone surface. As systems submitted to gravity field, a non-zero angular momentum induces an effective force in the radial direction. When friction is not relevant, the dynamics along the radial direction derives from a potential energy  $V(r) = \sqrt{\rho^2 + r^2} + J^2 / (4r^4)$  as  $(\dot{r}^2 / 2) + V(r) = E$ . Since the variable is oscillating in a potential well, the trajectory of the ball is therefore included in a circular strip of

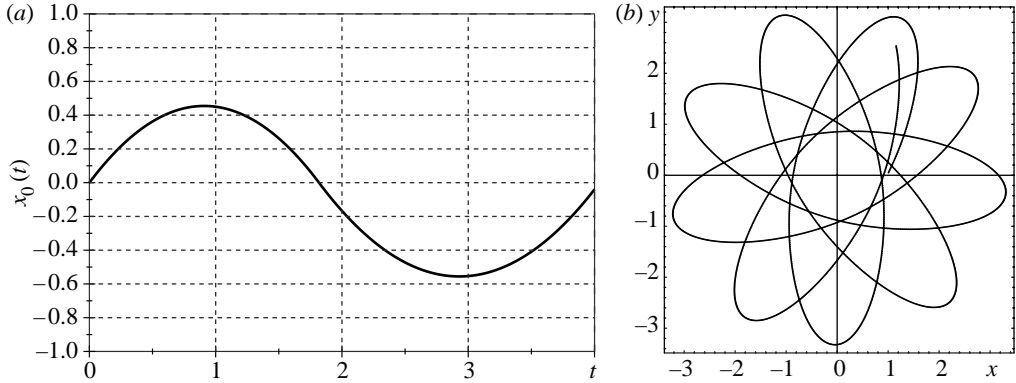


Figure 2. (a) Oscillatory solution obtained with  $\mu=0.1$ . (b) Rosace-like oscillation obtained with  $\mu=0$ .

the cone. The precession of the particle is reminiscent of the precession of a vertical pendulum due to either Earth's rotation as in Foucault experiment or the rotation induced by the intrinsic nonlinearities of the pendulum (see our recent study in Rousseaux *et al.* 2006).

Let us take the limit  $\rho \rightarrow 0$  in equation (3.1) and scale the time in order to make  $\tan \alpha$  disappear,

$$\ddot{A} = -\frac{A}{|A|} - \mu,$$

where  $\mu = \tan \theta / \tan \alpha$ . Thus, the ball is submitted to a force with a constant amplitude. This force is not central because the inclination induces an additional force in the  $x$ -direction (its amplitude is measured by  $\mu$ ). The above equation has the following symmetry:  $A \rightarrow B$  and  $t \rightarrow 1/\sqrt{B}$ . There exists a trivial solution that is equivalent to a free fall. Let us set  $y=0$ , then we have

$$\ddot{x} = -\text{sign}(x) - \mu.$$

The function  $\text{sign}(x)$  is not defined at the point  $x=0$ , and the above equation is singular at  $x=0$ . This reflects the fact that there is a shock when the ball passes at the origin, and this effect disappears by taking a finite value for  $\rho$ . Consequently, the oscillation is a composition of two distinct parabolas whose coefficients are related to the sign of  $x$ . Owing to the symmetry, we can choose without loss of generality that  $x(0)=0$  and  $\dot{x}(0) = 1$ , and then have the oscillation along the  $x$ -direction,

$$x_0(t) = -\frac{1}{2}(1 + \mu)t^2 + t, \quad 0 < t \leq \frac{2}{1 + \mu}, \tag{3.5}$$

$$x_0(t) = \frac{1}{2}(1 - \mu)t^2 - \frac{3 - \mu}{1 + \mu}t + \frac{4}{(1 + \mu)^2}, \quad \frac{2}{1 + \mu} < t \leq \frac{4}{1 - \mu^2}. \tag{3.6}$$

A typical temporal evolution of this trajectory is shown in figure 2a.

We have performed several numerical simulations for finite value of  $\rho$  and  $\mu$ , in order to explore the large phenomenology of chaotic behaviours displayed by the trajectory of a massive particle inside an inverted and inclined cone. Numerical computations are done with a fourth-order Verlet algorithm (1967) which preserves the energy of the system on average. The energy is usually fixed to the value  $\kappa = 1$ ,

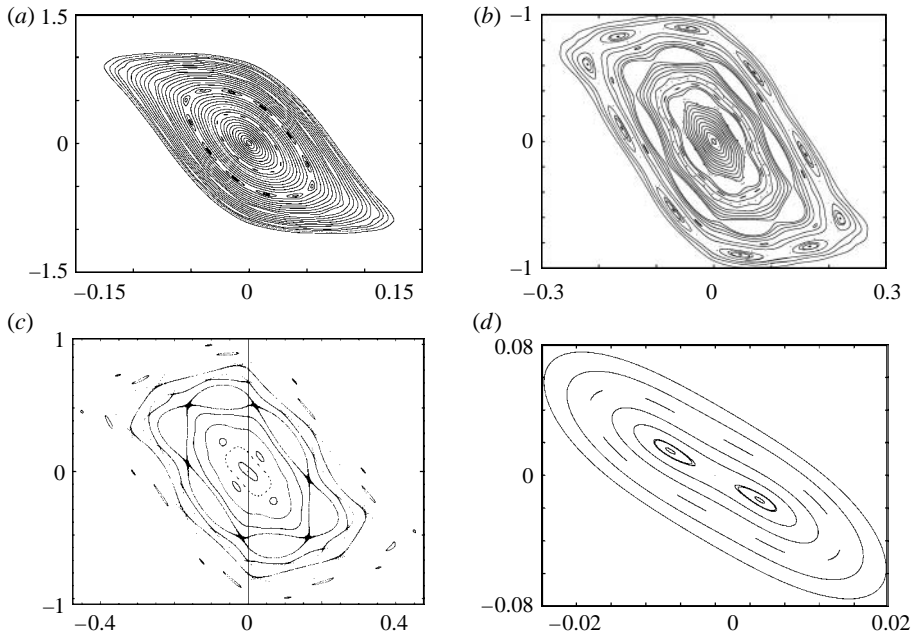


Figure 3. Poincaré sections taken at  $x=0$ : plane  $(y, \dot{y})$ . (a)  $\mu=0.1$  and  $\rho=0.01$ ; (b)  $\mu=0.2$  and  $\rho=0.01$ ; (c)  $\mu=0.3$  and  $\rho=0.01$ ; (d) zoom of (c) near the origin where the period-doubling instability appears clearly.

with  $\rho=0.01$  and the typical time-step of 0.01. For a gently tilted cone, the well-known behaviour of rosette-like trajectories is still present, as shown in figure 2*b*. But for large  $\mu$ , complex behaviour appears. In order to clarify where and how this complexity appears, a Poincaré section is performed at the point  $x=0$  using the Hénon algorithm (1982) as in a previous study by Lopez-Ruiz & Pacheco (2002).

As the parameter  $\mu$  is increased, islands appear on the Poincaré section denoting the presence of resonances, as shown in figure 3*c*, where homoclinic chaos developed (José & Saletan 1998). The oscillation along the  $x$ -direction remains marginally stable until a critical value of  $\mu$  (which depends on the regularization parameter  $\rho$ ), where a period-doubling bifurcation occurs as exhibited in figure 3*d*. In the real space, it is a ribbon whose arms cross in the most inclined part of the cone as shown in figure 4*a*; the extremities of the ribbon point downward in the direction of inclination. Moreover, one can observe trajectories with multiple periods if one explores the ‘islands’ in the Poincaré section far away from the origin (figure 3*c*). However, it happens that the extremities point in the opposite direction of the inclination with multiple periods (figure 4*b,c*) and the trajectory may be asymmetric (figure 4*c*) or chaotic (figure 4*d*).

#### 4. Linear stability analysis

In §3, we deduced the equations for the coordinates of the constrained ball inside a cone (equation (3.1)). In the limit of a small radius of curvature  $\rho$ , analytical solution can be obtained, but the system becomes highly singular. It appears that a critical tilt angle of the cone induces a period-doubling instability. In this

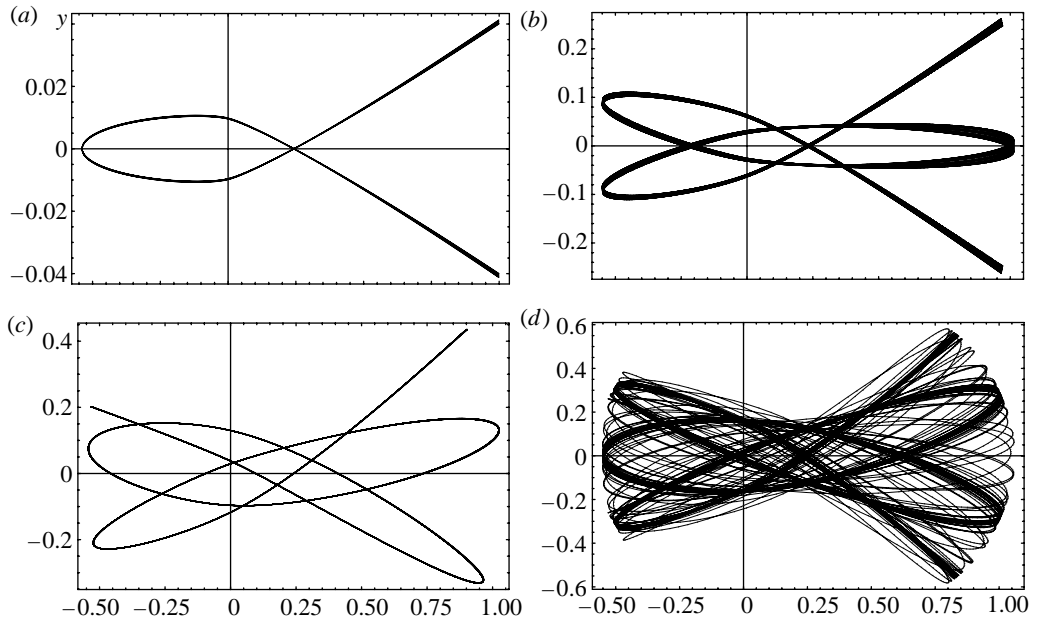


Figure 4. (a) Trajectory of the ball in the  $(x, y)$ -plane showing the period-doubling behaviour  $\rho=0.01$ . (b) A trajectory with a period four times higher than the trivial solution. (c) Asymmetric and (d) chaotic trajectory in the  $(x, y)$ -plane obtained with  $\mu=0.3$  and  $\rho=0.01$ .

section, we analyse the stability of the oscillation  $A=x_0(t)$  along the  $x$ -direction,  $x_0(t)$  being periodic with period  $T$ :  $x_0(t) = x_0(t + T)$ . We just need to study the dynamics of perturbations  $(u, v)$  with

$$x(t) = x_0(t) + \varepsilon u(t), \tag{4.1}$$

$$y(t) = \varepsilon v(t), \tag{4.2}$$

assuming that the amplitude of the perturbation  $\varepsilon$  is small. We then deduce the linearized system for the perturbations. The equations for  $u$  and  $v$  are decoupled,

$$\ddot{u} = -\frac{\rho^2}{(\rho^2 + x_0(t)^2)^{3/2}} u, \tag{4.3}$$

$$\ddot{v} = -\frac{1}{\sqrt{\rho^2 + x_0(t)^2}} v. \tag{4.4}$$

Since  $x_0(t)$  is periodic, it is necessary to construct the so-called monodromy matrix (Joseph & Iooss 1997), i.e. the mapping that describes how the perturbation evolves during one oscillation period  $T$ ,

$$\begin{pmatrix} u_{i+1} \\ \dot{u}_{i+1} \end{pmatrix} = L_u(T) \begin{pmatrix} u_i \\ \dot{u}_i \end{pmatrix}, \tag{4.5}$$

$$\begin{pmatrix} v_{i+1} \\ \dot{v}_{i+1} \end{pmatrix} = L_v(T) \begin{pmatrix} v_i \\ \dot{v}_i \end{pmatrix}, \tag{4.6}$$

where the indices  $w_j=w(t=jT)$ . The oscillation is stable if the perturbation decreases during the temporal evolution, i.e. when  $i \rightarrow \infty$ . Consequently, if  $L_u(T)^i$

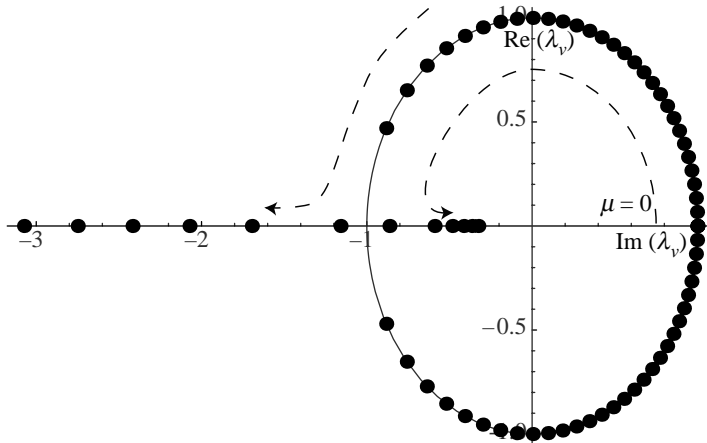


Figure 5. Movement of the Floquet multipliers in the complex plane as the control parameter  $\mu$  is varied. When  $\mu=0$ , both exponents are equal to 1. As  $\mu$  is increased, they move on the unit circle until they collide when they become equal to  $-1$ . Further augmentation of  $\mu$  pushes one of the Floquet multiplier outside the unit circle: the oscillation undergoes a period-doubling instability.

and  $L_v(T)^i$  remain bounded as  $i \rightarrow \infty$ , the system will be stable. It is then necessary to compute the eigenvalues  $\lambda_{u,v}$  of  $L_{u,v}(T)$ : the Floquet multipliers  $\lambda_{u,v}$ . As usual (Joseph & Iooss 1997), the stability of the oscillation will be related to the eigenvalues of  $\lambda_{u,v}$ . When a Floquet multiplier denoted  $\sigma$  becomes higher than one in absolute value, instability occurs, as  $\sigma^i$  will diverge as  $i \rightarrow \infty$ .

We constructed numerically the monodromy matrices  $L_u(T)$  and  $L_v(T)$ , by integrating the equations of motion with an energy-preserving algorithm: the Verlet method (fourth-order precise). The typical time-step is 0.01. The flow matrix is then computed numerically and its eigenvalues evaluated. It appears that the trivial oscillation ( $y=0$ ) becomes unstable if the cone is tilted with a sufficiently high angle as one Floquet multiplier becomes real and smaller than  $-1$ . The Floquet multipliers  $\lambda_u$  never give rise to an instability. In figure 5, the Floquet multipliers  $\lambda_v$  are plotted in the complex plane as the tilt parameter  $\mu$  is varied. When  $\mu=0$ , the two Floquet multipliers are equal to one and as  $\mu$  increases they move along the unit circle; this trajectory is imposed due to the Hamiltonian nature of the problem.

Therefore, the oscillation along the  $x$ -direction loses its stability via a period-doubling bifurcation. The instability threshold depends on the regularization radius  $\rho$  and we computed the dependence of this parameter: the critical angle (deduced from the parameter  $\mu$ ) is computed as a function of the radius of the origin of the cone (figure 6). We point out that the period doubling was calculated here only in the limit of small angle  $\alpha$ .

## 5. The experiments

We have built an inverted cone in aluminium with an angle  $\alpha=14^\circ$  with respect to the horizontal (figure 7).

The cone was mounted on a plate which can make an angle  $\beta$  with the horizontal plane. A vertical screw is coupled to a protractor and permits to



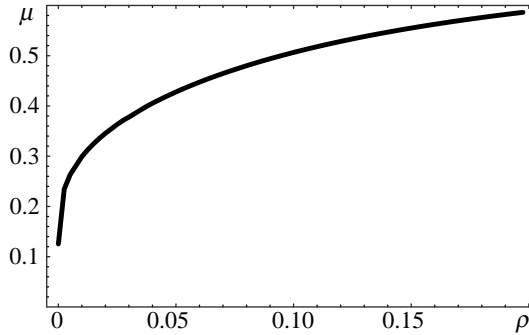


Figure 6. Curve of marginal stability of the oscillation in the  $x$ -direction as a function of the radius of the cone at the origin. There exists a critical angle  $\theta = \mu \tan \alpha$  for which the oscillation becomes unstable by a period-doubling scenario. We find  $\mu = 0.2992$  for  $\rho = 0.01$ .



Figure 7. Experimental set-up.

incline the plane. Depending on the way we turn the screw, we can increase or decrease the angle of the cone with respect to the direction of the gravitational field. The external radius of the cone as seen from above is 130 mm. The radius of the internal spherical regularization seen from above is 2.5 mm. Hence, the dimensionless radius  $\rho = 2.5/130 = 0.0192$ . We also use a latex ball of radius 2.2 cm. Hence, as the radius of the ball is higher than the regularization, it allows us to choose the radius of the sphere as the ‘cut-off’ and make an effective non-dimensional radius  $\rho = 2.2/13 = 0.16$ . The inclined plane with the inverted cone is fixed on a plate which can be ruled for the horizontality and verticality. From this plate, two vertical bars support a horizontal bar where we placed a CCD camera for visualization purposes and whose vertical position can be changed. The lighting is set close to the camera in order to light the cone from above. One records movies of the motion of a ball launched with no initial velocity from a point of the cone. Then, using image processing, we reconstruct the figures followed by the ball. The resolution for the lengths is 1 mm per pixel. For null inclination, we recover the usual precession as displayed by Nauenberg (2005b, fig. 10) with a stroboscopic procedure. It is rather easy experimentally to observe

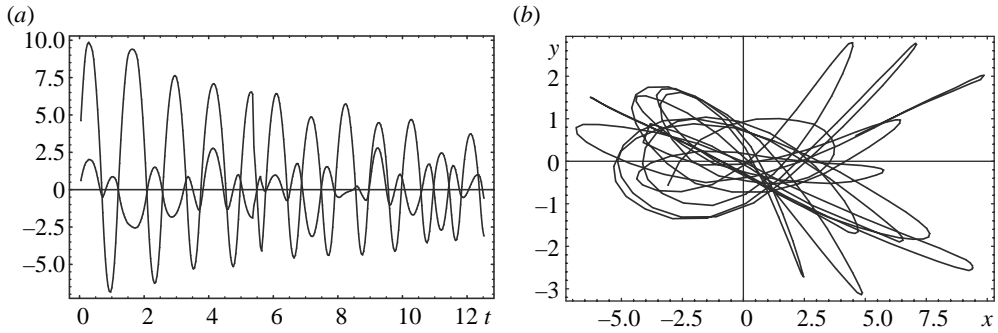


Figure 8. Experimental chaos ( $\alpha = 14^\circ - \beta = \alpha/2 = 7^\circ - \rho = 0.0192 - g = 9.81$ ). (a) Temporal evolution of the coordinates:  $x$  with grey curve and  $y$  with thick black curve. (b) Trajectory of the sphere in the  $(x, y)$ -plane.

by eye the period-doubling trajectory when one inclines the cone at roughly half its intrinsic angle when  $\rho$  is big enough, as predicted in figure 5. Finally, we can only guess that Robert Hooke encountered such chaotic motions as the one represented in figure 8.

## 6. Conclusions

To incline an inverted cone and let a ball move in it is sufficient in order to display a chaotic behaviour. We have shown using a parabolic regularization, in order to avoid shocks, that the motion of a particle in an inverted and inclined cone displays a transition to chaos with period doubling. We have observed both numerically and experimentally several complicated meanderings of the trajectory and have studied the stability of the motion. We speculate that Robert Hooke may have observed complicated movements while performing his analogue experiments in order to understand the planets' orbits simply owing to the fact that a small angle of the cone with respect to its support (a table for example) is sufficient sometimes to observe irregular motions.

It is rather strange that the development of modern chaos theory has made no references to such classic situations which are potentially unstable as the one described by Hooke. Maybe, the perfect beauty of the rosaces was more delightful for his century aesthetic criteria.

## References

- Patterson, L. D. 1952 Pendulums of Wren and Hooke. *Osiris* **10**, 277–321. (doi:10.1086/368556)
- Gal, O. 1996 Producing Knowledge in the workshop: Hooke's 'inflection' from optics to planetary motion. *Stud. Hist. Phil. Sci.* **27**, 181–205. (doi:10.1016/0039-3681(95)00035-6)
- Nauenberg, M. 2005 Curvature in orbital dynamics. *Am. J. Phys.* **73**, 340–348. (doi:10.1119/1.1842728)
- Nauenberg, M. 2005 Robert Hooke's seminal contribution to orbital dynamics. *Phys. Perspect.* **7**, 4–34. (doi:10.1007/s00016-004-0226-y)
- Routh, E. J. 1898 A treatise on dynamics of a particle. With numerous examples. Cambridge University Press, Cambridge, UK. (<http://name.umdl.umich.edu/ABR4374>)

- Lopez-Ruiz, R. & Pacheco, A. F. 2002 Movimiento de una partícula sobre la superficie de un cono invertido. *Anuario del Centro de la Universidad Nacional de Educación a Distancia en Calatayud* **1**, 127–143.
- Lopez-Ruiz, R. & Pacheco, A. F. 2002 Sliding on the inside of a conical surface. *Eur. J. Phys.* **23**, 579–589. (doi:10.1088/0143-0807/23/5/314)
- Lopez-Ruiz, R. & Pacheco, A. F. 2005 Registering seconds with a conic clock. *Chaos Solitons Fractals* **23**, 67–72. (doi:10.1016/j.chaos.2004.04.016)
- Bergé, P., Pomeau, Y. & Vidal, C. 1984 *Order within chaos: towards a deterministic approach to turbulence*. New York, NY: Wiley.
- José, J. V. & Saletan, E. J. 1998 *Classical dynamics: a contemporary approach*. Cambridge, UK: Cambridge University Press.
- Rousseaux, G., Coulet, P. & Gilli, J. M. 2006 Robert Hooke's conical pendulum from the modern viewpoint of amplitude equations and its optical analogues. *Proc. R. Soc. A* **462**, 531–540. (doi:10.1098/rspa.2005.1587)
- Verlet, L. 1967 Computer “experiments” on classical fluids. I. Thermodynamical properties of Lennard-Jones molecules. *Phys. Rev.* **159**, 98–103. (doi:10.1103/PhysRev.159.98)
- Hénon, M. 1982 On the numerical computation of Poincaré maps. *Phys. D* **5**, 412–414. (doi:10.1016/0167-2789(82)90034-3)
- Joseph, D. D. & Iooss, G. 1997 *Elementary stability and bifurcation theory*. Berlin, Germany: Springer.